Zirconium Phosphate-Methylene Blue Composite Immobilized at Room-Temperature Ionic Liquid Matrix for Electrochemical Detection of NADH

[1]XIAOYING ZENG, [1]JUXING JIANG, [2]HAIYUN ZHANG, [2]WENJING LU AND [2]DAWEI PAN *

[1]*R&D Center, HongyunHonghe Tobacco (Group) Co, LTD, Kunming, 650202, P.R. China.*
[2]*Key Laboratory of Coastal Zone Environmental Processes and Ecological Remediation, Yantai Institute of Coastal Zone Research(YIC), Chinese Academy of Sciences(CAS); Shandong Provincial Key Laboratory of Coastal Zone Environmental Processes, YICCAS, Yantai Shandong 264003, P.R. China.*
dwpan@yic.ac.cn*

Summary: Electroactive methylene blue (MB) entrapped in α-zirconium phosphate (ZrP) were first synthesized by a simple chemical method. Room-temperature ionic liquid (IL) was used as a matrix to immobilize ZrP-MB composite on pyrolytic graphite (PG) electrode and the resulting modified electrode can be utilized in electrocatalytic oxidation of NADH. Because of the combination of the excellent electroactivity of MB, the good chemical and mechanical properties of ZrP and the good ionic conductivity of IL, the response current of NADH at PG/ZrP-MB/IL electrode is much larger than that in bare and ZrP-IL electrode and the interference of ascorbic acid can be avoided efficiently. The PG/ZrP-MB/IL electrode displayed high sensitivity (76.5 mA M^{-1} cm^{-2}), low detection limit (6 μM), fast response time (within 5s) and wide linear range (6-540 μM).

Introduction

A series of organic dyes , such as methylene blue (MB), methylene green, Prussian blue, phenazines and thionin, etc, have been used in chemically modified electrode and all displayed excellent mediating ability in electrocatalysis [1-3]. Methylene blue, a typical cationic dye whose electrochemical properties are well known in the solution phase, has been used as a redox indicator in biocatalysis and biosensor because it can largely decrease the overpotential of electroactive species and prevent fouling of the electrode surface [4, 5]. However, such low molecular weight soluble mediator is disadvantageous in practical application as it can leach out of the electrode, which may lead to a significant signal loss and affect the stability of electrodes [6].

The metal salts of phosphoric acid have been known for over a century. In the last 40 years, they have been the object of continuous interest in the chemical literature [7, 8]. According to the literature, when the molar ratio of phosphate to zirconium is greater than two, the product of the precipitation is small crystalline particles of α-zirconium phosphate (ZrP) [7]. Moreover, as a good support, an ion exchanger and an excellent acid catalyst, zirconium phosphate has taken considerable attention to wide applications such as dehydration of cyclohexanol, dehydrogenation of cyclohexene, ethylene and methanol oxidation, etc. But the practical application of ZrP in electrochemical research is a matter of concern because of its poor solubility in water or organic solvent.

Additionally, room-temperature ionic liquids (ILs) are ionic media resulting from the combination of organic cations and various anions. They are liquids at room temperature and represent a new class of non-aqueous but polar solvents that are able to dissolve many compounds. Because of their unique chemical and physical properties, ionic liquids have been paid considerable attention in the past such as high chemical and thermal stability, negligible vapor pressure and high conductivity [9]. Recently, one important application of ILs is as a matrix to incorporate with conventional materials such as cellulose [10], carbon materials [11, 12], and sol-gel-based silica [13].

Until now, only a few literatures about the electroanalysis application of organic–inorganic composite have been reported [14, 15]. In this paper, a novel organic–inorganic composite combining the efficient electrocatalytic properties of MB with good mediator support ZrP was synthesized. One kind of ILs was used as a matrix to immobilize the ZrP-MB composite and the resulting modified electrode can be used for electrochemical detection of NADH. The response current of NADH at ZrP-MB/IL modified electrode is much larger than that in bare and ZrP/IL modified electrode at low potential. Additionally, the α-ZrP-MB-IL modified electrode shows the good anti-interference of ascorbic acid and excellent cycling stability.

Results and Discussion

Characterization of ZrP-MB Composite

Fig. 1 shows the UV spectra of ZrP, MB and

ZrP-MB composite. ZrP has no absorption peak in the range of 300-800 nm (curve a), but MB aqueous solution has two characteristic absorption peaks (curve b). One sharp peak at around 664 nm is the characteristic of the MB monomer in solution [16]. Another wide peak at 616 nm is ascribed to the absorbance of the MB dimmer in solution [17]. The chemisorption of MB onto ZrP was evident from the spectrum of the ZrP-MB composite (curve c), which is similar to that of the free MB. There is a little change in the spectrum of MB after its adsorption onto the ZrP. Two absorption peaks of free MB at 664 and 616 nm are shifted to 662 and 617 nm, respectively. Additionally, the FTIR spectra of ZrP, MB and ZrP-MB composite were also investigated and the corresponding results are shown in Fig. 2. The FTIR spectrum of free MB exhibits its ring stretch at 1601 cm^{-1}, the symmetric stretch of C-N at 1396 cm^{-1}, and symmetric deformation of -CH_3 at 1354 cm^{-1} (not shown). The FTIR spectra of the ZrP (Fig. 2a) has five characteristic peaks at 1626, 1384, 1251, 1045, 964 cm^{-1}, which accord with similar with the reported [8] Five peaks at 1626, 1384, 1251, 1045, 964 cm^{-1}, which are the characteristic peaks of ZrP [8], can be observed on FTIR spectra of the synthesized ZrP (Fig. 2a). Similar to the conclusion drawn from the UV-vis spectra, the adsorption of MB onto the ZrP was also substantial. Compared with the spectrum of ZrP, at the spectrum of ZrP-MB composite (Fig. 2b), the peaks at 964 and 1252 cm^{-1} disappeared and a new peak at 1401 cm^{-1} appeared. The peaks at 1045, 1626 and 2346 cm^{-1} were shifted to 1067, 1631 and 2404 cm^{-1}. These imply the strong interaction between MB and ZrP.
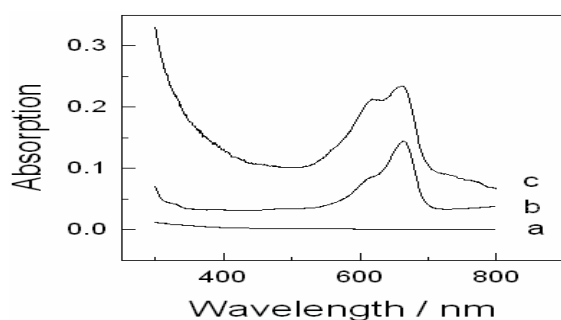

Fig. 1:   UV-vis spectra of (a) ZrP, (b) MB and (c) ZrP-MB composite.

The cyclic voltammograms of bare PG electrodes with and without ZrP-MB/bmimPF$_6$ modification in 0.067 M phosphate buffer solution (pH 7.0) aqueous solutions are presented in Fig. 3. No redox peaks can be observed at the PG and

PG/ZrP/bmimPF$_6$ electrode while a reversible redox peak can be observed clearly at the PG/ZrP-MB/bmimPF$_6$ electrode. The formal potential $E_{1/2}$ for the peak is -0.28 V and the corresponding peak potential separation is 140 mV. The shape of the curves and the peak potentials is ascribed to the electrochemical behavior of MB.
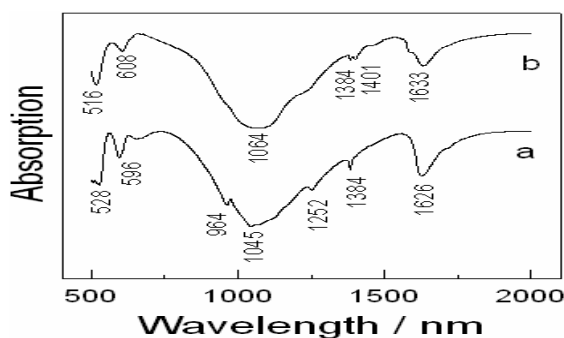

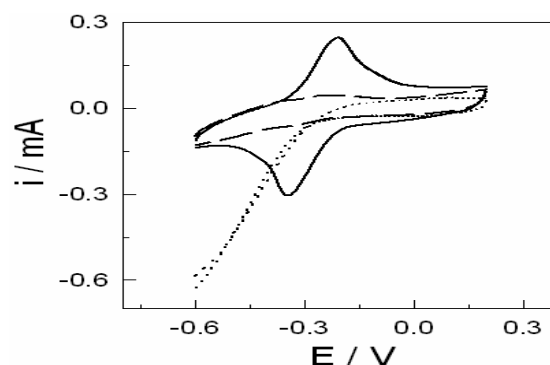Fig. 2:   FTIR spectra of (a) ZrP, (b) ZrP-MB composite.

Fig. 3:   Cyclic voltammograms of the PG (dotted line), PG/ZrP/bmimPF$_6$ (dashed line) and PG/ZrP-MB/bmimPF$_6$ electrode (solid line) in a 0.067 M phosphate buffer solution (pH 7.0). Scan rate, 50 mV s^{-1}.

Electrocatalytic Oxidation of NADH at PG/ZrP-MB/bmimPF$_6$ modified Electrode

To discern the role of individual components and their possible affection on electrocatalysis of NADH, response currents to the oxidation of NADH at kinds of modified electrodes in 0.067M phosphate buffer solution (pH 7.0) were shown in Fig. 4. At 0.0 V, the much small anodic response to NADH can be detected at bare PG and PG/ZrP/bmimPF$_6$ electrode, which indicates PG support, ZrP film as well as IL film play the role of electrochemical inaction structural matrix at low applied potential. However,

at PG/ZrP-MB/bmimPF$_6$ electrode, a relatively large response current can be obtained. The enhancement of the response current may be the reasons as follows: (I) the existence of MB cause the decrease of the detection potential of NADH. (II) ZrP-MB composite in bmimPF$_6$ matrix result in the improvement of the electronic and ionic transport capacity.
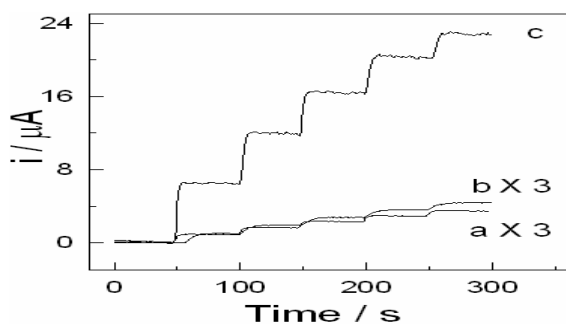

Fig. 4: i-t curves of (a) PG, (b) PG/ZrP/bmimPF$_6$ and (c) PG/ZrP-MB/bmimPF$_6$ electrode to addition of 0.5 mM NADH in 0.067 M phosphate buffer solution (pH 7.0).

Fig. 5 presents an amperometric trace recorded at PG/ZrP-MB/bmimPF$_6$ electrode at 0.0 V in a stirred 0.067 M phosphate buffer solution (pH 7.0), which was spiked with aliquots of NADH stock solution. The current flowing through the electrode increased in a stepwise manner after each addition of NADH. High sensitivity (76.5 mA M^{-1} cm^{-2}), low detection limit (6 μM NADH at S/N=3), fast response time (within 5s) and wide linear range (6-540 μM, r = 0.995) can be obtained at the PG/ZrP-MB/bmimPF$_6$ electrode. These characters are same or better than those reported [18, 19]. On the other hand, The PG/ZrP-MB/bmimPF$_6$ electrode has good anti-interference ability to AA because AA can not be oxidized at so low potential and the Nafion film can prevent AA close to the electrode. The long-term cycle stabilities of PG/ZrP-MB/bmimPF$_6$ electrode have also been studied by continuous cycling. When the cycle number is 100, only 7% loss of the electrochemical activity of the PG/ZrP-MB-bmimPF$_6$ electrode can be observed. This implies that MB absorbed on ZrP in bmimPF$_6$ matrix and entrapped in Nafion membrane can effectively diminish the loss of MB from electrode.

Experimental

Reagents and Apparatus

MB, zirconyl chloride and phosphoric acid were purchase from Chemical Reagent Company of Shanghai, China. Water-immiscible and biocompatible ILs used in this study is 1-butyl-3-methylimidazolium hexafluorophophate (bmimPF$_6$). NADH (in the form of sodium salt, >92% purity) was purchased from Shanghai Lizhu Dongfeng Biotechnology Co. Ltd., China. All other reagents were of analytical grade and were used without further purification. Double-distilled water was used throughout.
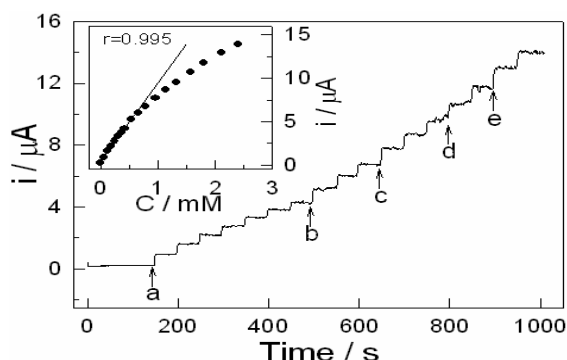

Fig. 5: i-t curve of PG/ZrP-MB/bmimPF$_6$ electrode to addition of (a) 0.06, (b) 0.12, (c) 0.18, (d) 0.24 and (e) 0.30 mM NADH in 0.067 M phosphate buffer solution (pH 7.0) at 0.0 V. Inset is the calibration curve of the response current of PG/ZrP-MB/bmimPF$_6$ electrode to NADH concentration.

Cyclic voltammetry measurements were carried out in a conventional three-electrode cell controlled by CHI 660D Electrochemical Work Station (CH Instruments, Inc). Pyrolytic graphite (PG) electrode (surface area 0.12 cm^2) was used as working electrode. A platinum foil was applied as the counter electrode and a saturated calomel electrode (SCE) served as reference electrode. All potential values given below refer to SCE. All experiments were performed at room temperature.

The UV/Vis spectrum of ZrP-MB composite was recorded with a DU 800 spectrophotometer (Beckman, USA). The ZrP-MB adduct was pressed into a KBr pellet for FTIR investigation (WQF-410 spectrometer, Beijing, China).

Preparation of ZrP-MB Composite and PG/ZrP-MB/bmimPF$_6$ Modified Electrode

The preparation of ZrP-MB composite is similar to the preparation of ZrP reported in

literatures [7, 8]. In brief, 1.95g zirconyl chloride is dissolved in 50 ml 2M HCL. This solution is slowly added to 25 ml 1.25M H_3PO_4 solution containing 2mg/ml MB with strong stirring (initial P/Zr ratio 3.6). The precipitate is filtered and washed with 0.3M H_3PO_4 solution till free from chloride ion. The dark-blue solid is dried in a vacuum at room temperature. As compared, the solid of ZrP is prepared in the similar manner without using MB.

2 mg ZrP-MB particles mixed with 5μL pure bmimPF$_6$ were ground with an agate mortar for about 30 min, and a dark-blue gel was formed, which is similar to the black IL-CNT gel [12]. Meanwhile, PG electrode was polished with alumina, followed with being washed in double-distilled water and ethanol, respectively, then activated by sweeping in 0.5 M H_2SO_4 for almost 20 cycles. Then, the PG electrode was rubbed over the gel placed on a smooth glass slide for almost 15 min, and the ZrP-MB/bmimPF$_6$ gel was mechanically attached to the electrode surface. After the gel on the electrode surface was smoothed with a spatula to leave a thin gel film on the PG electrode surface. Finally, 0.5 wt% Nafion solution was cast on the surface of the resulting electrode.

Conclusion

Immobilization of electroactive MB is introduced by the entrapment of MB in α-zirconium phosphate (ZrP) were first synthesized by a simple chemical method. The physical and chemical properties of composite were investigated in detail. Room-temperature ionic liquid (IL) was used as a matrix to immobilize ZrP-MB composite on pyrolytic graphite electrode (PG) and the resulting modified electrode can be utilized in electrocatalytic oxidation of NADH. Because of the combination of the excellent electroactivity of MB, the good chemical and mechanical properties of ZrP and the good ionic conductivity of IL, the response current of NADH at PG/ZrP-MB/IL electrode is much larger than that in bare and ZrP-IL electrode and the interference of ascorbic acid can be avoided efficiently. The PG/ZrP-MB/IL electrode displayed high sensitivity (76.5 mA M^{-1} cm^{-2}), low detection limit (6 μM NADH at S/N=3), fast response time (within 5s) and wide linear range (6-540 μM, r = 0.995). The unique material based on electroactive composite and ionic liquid has great potential applications in electrocatalysis and chemo/bio-sensors.

Acknowledgements

References

1. A. A. Karyakin, E. A. Puganova, I. A. Budashov, I. N. Kurochkin, E. E. Karyakina, V. A. Levchenko, V. N. Matveyenko and S. D. Varfolomeyev, *Analytical Chemistry*, **76**, 474 (2004).
2. M. Arvand, S. Sohrabnezhad, M. F. Mousavi, M. Shamsipur and M. A. Zanjanchi, *Analytica Chimica Acta*, **491**, 193 (2003).
3. S. A. John and R. Ramaraj, *Journal of Electroanalytical Chemistry*, **561**, 119 (2004).
4. G. L. Xue, J. Xiong, H. L. Guo, G. L. Cao, S. S. Nie and H. M. Hu, *Electrochimica Acta*, **69**, 315 (2012).
5. J. L. Wang, A. Munir, Z. H. Li and H. S. Zhou, *Talanta*, **81**, 63 (2010).
6. H. Yao, N. Li, S. Xu, J. Xu, J. Zhu and H. Chen, *Biosensors and Bioelectronics*, **21**, 372 (2005).
7. C. Trobajo, S. A. Khainakov, A. Espina and J. R. Garcia, *Chemistry of Materials*, **12**, 1787 (2000).
8. S. De, A. De, A. Das and S. K. De, *Materials Chemistry and Physics*, **91**, 477 (2005).
9. T. Welton, *Chemical Reviews*, **99**, 2071 (1999).
10. M. B. Turner, S. K. Spear, J. D. Holbrey and R. D. Rogers, *Biomacromolecules*, **5**, 1379 (2004).
11. T. Fukushima, A. Kosaka, Y. Ishimura, T. Yamamoto, T. Takigawa, N. Ishii and T. Aida, *Science*, **300**, 2072 (2003).
12. F. Zhao, X. Wu, M. Wang, Y. Liu, L. Gao and S. Dong, *Analytical Chemistry*, **76**, 4960 (2004).
13. Y. Liu, M. Wang, J. Li, P. He, H. T. Liu and J.H. Li, *Chemical Communications*, 1778 (2005).
14. C. A. Borgo, A. M. Lazarin and Y. Gushikem, *Sensors and Actuators* B*: Chemical*, **87**, 498 (2002).
15. F. D. Munteanu, N. Mano, A. Kuhn and L. Gorton, *Journal of Electroanalytical Chemistry*, **564**, 167 (2004).
16. Y. Yan, M. Zhang, K. Gong, L. Su, Z. Guo and L. Mao, *Chemistry of Materials*, **17**, 3457 (2005).
17. T. Sagara and K. Niki, *Langmuir*, **9**, 831 (1993).
18. M. Zhang and W. Gorski, *Analytical Chemistry*, **77**, 3960 (2005).
19. M. Zhang and W. Gorski, *Journal of the American Chemical Society*, **127**, 2058 (2005).